Constructing Functional Mesostructured Materials from Colloidal Nanocrystal Building Blocks

DELIA J. MILLIRON,* RAFFAELLA BUONSANTI, ANNA LLORDES, AND BRETT A. HELMS

Lawrence Berkeley National Laboratory, Berkeley, California 94720, United States

RECEIVED ON MAY 14, 2013

CONSPECTUS

Through synthesizing colloidal nanocrystals (NCs) in the organic phase, chemists gain fine control over their composition, size, and shape. Strategies for arranging them into ordered superlattices have followed closely behind synthetic advances. Nonetheless, the same hydrophobic ligands that help their assembly also severely limit interactions between adjacent nanocrystals. As a result, examples of nanocrystal-based materials whose functionality derives from their mesoscale structure have lagged well behind advances in synthesis and assembly.
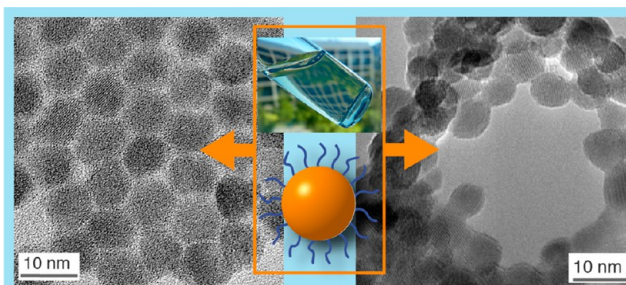
In this Account, we describe how recent insights into NC surface chemistry have fueled dramatic progress in functional mesostructures. In these constructs, intimate contact between NCs as well as with heterogeneous components is key in determining macroscopic behavior. The simplest mesoscale assemblies we consider are networks of NCs constructed by in situ replacement of their bulky, insulating surface ligands with small molecules. Transistors are a test bed for understanding conductivity, setting the stage for new functionality. For instance, we demonstrated that by electrochemically charging and discharging networks of plasmonic metal oxide NCs, the transmittance of near infrared light can be strongly and reversibly modulated.

When we assemble NCs with heterogeneous components, there is an even greater potential for generating complex functionality. Nanocomposites can exhibit favorable characteristics of their component materials, yet the interaction between components can also have a strong influence. Realizing such opportunities requires an intimate linking of embedded NCs to the surrounding matrix phase. We accomplish this link by coordinating inorganic anionic clusters directly to NC surfaces. By exploiting this connection, we found enhanced ionic conductivity in Ag_2S-in-GeS_2 nanocrystal-in-glass electrodes. In another example, we also found enhanced optical contrast when linking electrochromic niobium oxide to embedded tin-doped indium oxide (ITO) NCs. These dramatic effects emerge from reconstruction of the inorganic glass immediately adjacent to the NC interface.

When co-assembling NCs with block copolymers, direct coordination of the polymer to NC surfaces again opens new opportunities for functional mesoscale constructs. We strip NCs of their native ligands and design block copolymers containing a NC tethering domain that bonds strongly, yet dynamically, to the resulting open coordination sites. This strategy enables their co-assembly at high volume fractions of NCs and leads to well-ordered mesoporous NC networks. We find these architectures to be exceptionally stable under chemical transformations driven by cation insertion, removal, and exchange.

These developments offer a modular toolbox for arranging NCs deliberately with respect to heterogeneous elements and open space. We have control over metrics that define such architectures from the atomic scale (bonding and crystal structure) through the mesoscale (crystallite shapes and sizes and pore dimensions). By tuning these parameters and better understanding the interactions between components, we look forward to boundless opportunities to employ mesoscale structure, in tandem with composition, to develop functional materials.

Introduction

Chemical methods for growing nanocrystals (NCs) in solution phase have achieved remarkable sophistication, leading to the elucidation of size- and shape-dependent properties ranging from phase stability to luminescence and catalysis. Thanks to ever-advancing synthetic mastery
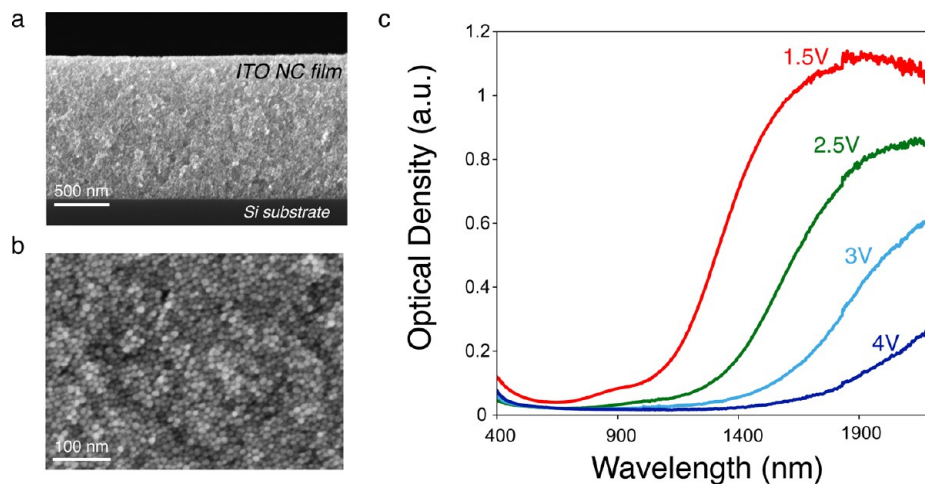
FIGURE 1. Plasmonic electrochromism of ITO NC networks. (a) Cross-sectional and (b) top-view scanning electron micrographs (SEM) of the networks. (c) Electrochromic response (i.e., optical switching upon electrochemical charging/discharging) of an ITO NC network on glass. Voltages are referenced to Li/Li⁺. Panel (c) adapted from ref 15. Copyright 2011 American Chemical Society.

over morphology and composition, exquisitely controlled NCs are now readily available to use as building blocks in the deliberate construction of functional materials and systems. The properties of these assemblies derive from those of their nanoscopic components but equally depend on the arrangement and bonding of those elementary units.

Almost as soon as synthetic methods emerged for the synthesis of highly uniform colloidal NCs, their proclivity for assembling into superlattices exhibiting long-range order was recognized. Soon after reporting the synthesis of near monodisperse CdSe NCs,[1] the Bawendi group published compelling electron micrographs of highly ordered close-packed superlattice assemblies.[2] Since then, the multiplicity of forces at play in such assembly processes have been investigated. Although hard sphere packing models could be used to rationalize some aspects of NC assembly,[3-6] ligand−ligand dispersion forces also play a central role.[7-9] And yet, these same ligands ultimately limit the functionality achievable in the resulting mesostructured materials. The ligands separate the inorganic cores, typically by 1 to 3 nm, restricting electronic and magnetic coupling and confining interparticle interaction primarily to longer range energy transfer processes.[7,8] Attempts to thermally decompose the ligands, post-assembly, met with some success in creating functional materials. For example, Black and co-workers studied the magnetoresistive properties of cobalt NC arrays in which the ligands had been thermally degraded to leave more conductive carbonaceous residue.[10] However, this strategy is only applicable to NCs with sufficient thermal stability, and ultimately the composition and bonding at the NC interfaces is neither controlled nor well understood.

These limitations have motivated the recent development of in situ chemical strategies to displace the native ligands with small molecules post-assembly.

Ligand Displacement to Form Nanocrystal Networks. The "native" ligands that coordinate NC surfaces provide steric stabilization in organic solvents, facilitating assembly and deposition of uniform films. These bulky ligands can then be replaced simply by soaking a thin-film NC assembly in a solution of small, surface-coordinating molecules. The development of such in situ ligand exchange strategies has brought about a renaissance in NC-based electronic materials; device performance characteristics previously arrived at through high temperature annealing have been met or even exceeded.

For example, in thin film transistors (TFTs), PbSe NC films soaked in a hydrazine solution exhibited electron mobilities approaching 1 cm²/V s with no further processing.[11] This mobility replicated that found earlier in TFTs of CdSe NCs printed with weakly bound ligands then annealed at 350 °C, and even after annealing, extreme hysteresis was reported, possibly reflecting poor electronic passivation of the surface.[12] Likewise, NC photovoltaic cells fabricated by exchanging the oleate ligands on lead sulfide NCs for 3-mercapto-proprionate have achieved power conversion efficiencies exceeding 5%,[13] well-exceeding the 2.9% efficiency of earlier CdTe cells sintered at 400°C.[14]

Substantial volume contraction accompanies ligand replacement, so in situ processing results in a largely random network of NCs with significant porosity. Each NC is connected to a variable number of neighbors, thus facilitating electronic conduction by hopping, and in some cases the
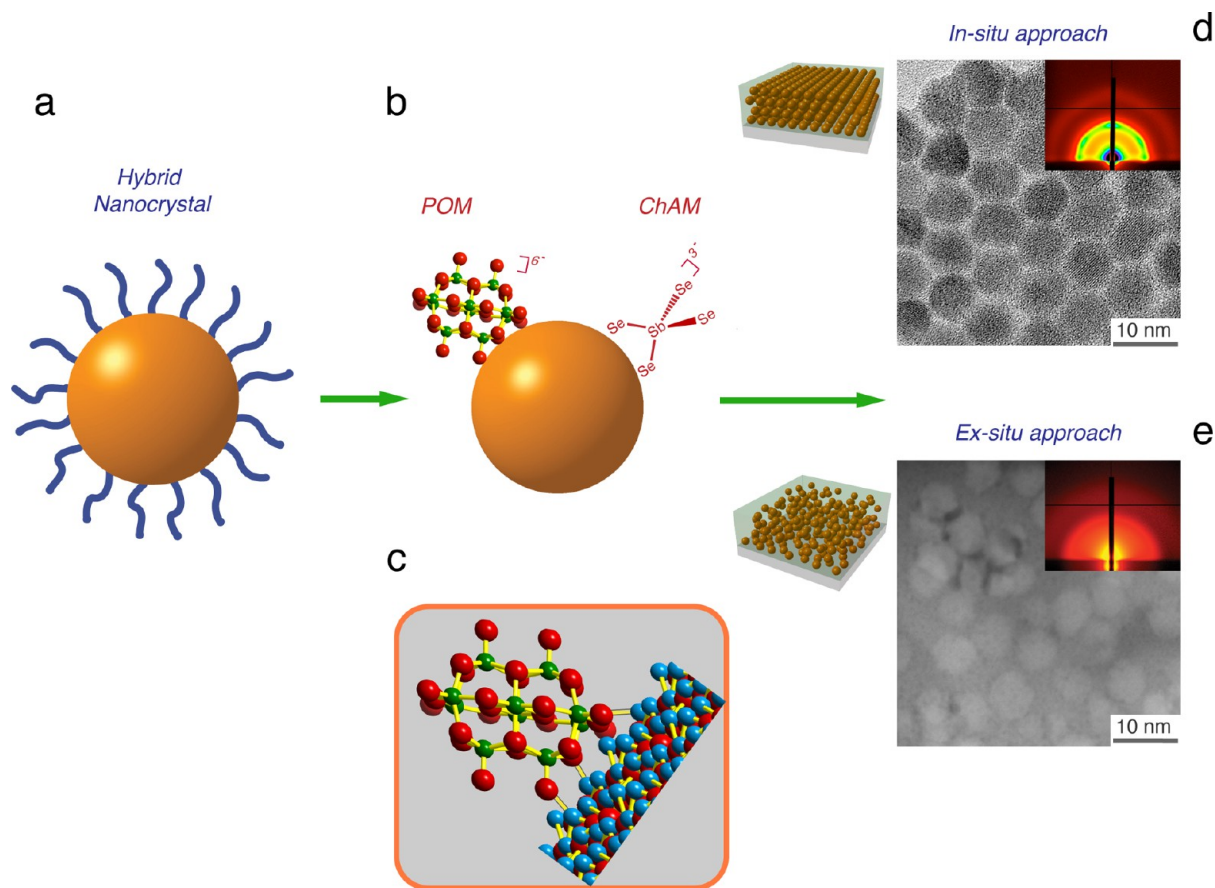
FIGURE 2. Synthesizing nanocrystal-in-glass composites by ligand exchange. (a) Native ligands are exchanged by inorganic molecular clusters: (b) polyoxometalates or chalcogenidometallates. (c) These clusters are chemically bonded to the NC, as shown schematically for a POM (i.e., $[Nb_{10}O_{28}]^{6-}$), at a NC surface (i.e., In_2O_3). Niobium atoms are in green, oxygen in red, and indium in blue. (d) Transmission electron micrograph (TEM) and grazing incidence small-angle X-ray scattering (GISAXS) of PbSe-in-SbSe$_x$. (e) Dark field scanning TEM and GISAXS of ITO-in-NbO$_x$. [Llordes, A.; Hammack, A. T.; Buonsanti, R.; Tangirala, R.; Aloni, S.; Helms, B. A.; Milliron, D. J. *J. Mater. Chem.* **2011**, *21*, 11631−11638] - Reproduced by permission of The Royal Society of Chemistry.

open network mesostructure is advantageous. For instance, we recently formed conducting networks of tin-doped indium oxide (ITO) NCs (Figure 1, panels a and b) by ligand exchange with formic acid, which is subsequently removed through thermal annealing (250 °C).[15] Electrons could be reversibly injected and extracted throughout the ITO NC network (in an electrochemical cell), thereby dramatically modulating the plasmon resonance absorption (Figure 1c). Notably, the porosity resulting from in situ ligand exchange enables penetration by the electrolyte even in micrometer thick films.[16]

For purely electronic devices like TFTs, higher density networks are preferable since the number of nearest neighbors to each NC is increased. For these applications, ex situ ligand exchange strategies, in which the native ligands are replaced by small molecules in the solution phase before depositing films, can be advantageous. However, small molecules, like hydrazine, are not generally capable of providing steric stabilization, so ionic ligands are used that can instead produce charge-stabilized NC dispersions. For instance, thiocyanate-terminated CdSe NC TFTs had mobilities around 20 cm^2/V s, while ex situ exchange with $[In_2Se_4]^{2-}$ gave a mobility of ∼15 cm^2/V s (both annealing at 200−250°C).[17,18] The latter is an example of a chalcogenidometallate cluster (ChAM).[19,20] ChAMs are a class of anionic inorganic molecules that can be synthesized by reductive dissolution of the parent metal chalcogenide compound;[21] they can act as coordinating ligands, introduced to NC surfaces through ex situ or in situ exchange.[22,23] But beyond acting as simple ligands, their tendency to condense upon annealing to form extended metal chalcogenide materials[21] suggests an opportunity to form an inorganic matrix surrounding the NCs.

NCs Embedded in Inorganic Hosts. Inspired by the unique optoelectronic properties of epitaxial quantum well and so-called self-assembled quantum dot heterostructures,

researchers made early attempts to embed colloidal semi-conductor NCs into host semiconductor matrices. Soon after CdSe NCs were first synthesized, Danek et al. pioneered the use of electrospray organometallic chemical vapor deposition to codeposit CdSe NCs with ZnSe matrix precursors.[24] However, the best-known method at the time for removing native ligands (stripping by mass action with pyridine) is not completely effective, leading to NC agglomeration. Later, Woggon et al. demonstrated that ZnSe could be overgrown epitaxially by molecular beam epitaxy to surround colloidal CdSe NCs, which were again deposited from pyridine solution.[25] However, the photoluminescence efficiency was low and the optical properties unstable, reflecting the poor electronic quality of the NC−matrix interface.

Recently, methods for quantitative removal and replacement of ligands have progressed markedly, allowing the development of new, robust strategies for embedding NCs in all variety of matrix materials. We have particularly focused on the use of ChAMs and polyoxometalate clusters (POMs) as precursors to amorphous metal chalcogenide and metal oxide matrix materials, respectively.[23,26] These inorganic clusters can be introduced through direct replacement of the native ligands or following reactive ligand stripping. In either case, direct bonds are made between clusters and NCs, and these bonds are retained in the eventual composite, creating an intimate linkage between the matrix and the embedded NCs. As a consequence, nanocrystal-in-glass composites exhibit functional characteristics strongly influenced by interfacial interactions.[27,28]

Our nanocrystal-in-glass approach offers excellent control of structure at multiple length scales (e.g., atomic, nano-, and meso-), as well as mixing and matching desired component compositions (Figure 2). Conventional methods do not offer this level of modularity, since they rely on thermally induced phase separation and in situ crystallization.[29] Precipitation of nanocrystalline domains typically occurs in a narrow segment of the time−temperature parameter space, inevitably leading to poor structural tunability (e.g., NC size) and compositional control. For complex stoichiometries, like doped materials, finding conditions that induce phase segregation and selective crystallization becomes a nearly impossible task. Such compositions can, however, be easily accessed by using colloidal NCs that are synthesized independently, then chemically linked to the matrix material. The interface area and nanocrystalline domain size become easily tunable parameters. Besides providing a route to new functional materials, this strategy offers a great opportunity to perform systematic studies on interface reconstruction,[28]

a key factor in determining mesoscale behavior that remains underexplored at crystal−glass interfaces.

Embedding colloidal NCs within inorganic amorphous materials can be accomplished by exchanging the native organic ligands with anionic ChAMs or POMs, which are charge balanced by small organic cations like tetramethyl-ammonium or hydrazinium.[22,23] The first demonstrations of such ligand exchange processes involved ChAMs and metal chalcogenide NCs.[22,23] Recently, we demonstrated that metal oxide nanocrystal-in-glass materials can be chemically constructed by related methods, using metal oxide colloidal NCs and POMs as the building units.[26] ChAMs and POMs can be coordinated by direct ligand exchange or, more generally, by first removing the native ligands using new reactive stripping strategies.[30,31] Linking processes can therefore be classified as a one-step or two-step, as well as in situ or ex situ. In any case, after ligand exchange, thermal annealing induces condensation of the clusters and decomposes their organic counterions. This process forms a continuous and purely inorganic matrix material (i.e., metal chalcogenide or metal oxide) to which the embedded NCs are covalently bonded.

In situ approaches typically follow a one-step process in which the native ligands are exchanged by mass action while soaking a self-assembled NC film in a solution containing the ChAMs or POMs.[23,26] Polar solvents (e.g., ethanol-amine or ethanol/water mixtures) are used to dissolve the anionic clusters and also solvate the native ligands as they are displaced. After rinsing the excess ligands, thermal annealing (at temperatures between 180 and 400 °C, depending on the composition) results in an amorphous inorganic matrix confined between the closely packed NCs, which retain the regular ordering inherited from the original assembly (Figure 2d). This approach is general to metal chalcogenide and metal oxide compositions and can readily yield ordered nanocomposites with high specific interface area (e.g., 0.92 nm^{-1}). However, to balance the contribution of each component (NCs and matrix) to the macroscopic properties we need to vary the volume fraction. Likewise, systematic variations of the specific interface area are essential to understand the emergence of interface reconstruction and its role in mesoscale behavior.

This tunability can be achieved by linking NCs and inorganic clusters in solution. Kovalenko et al. used ChAMs in a one-step, ex situ ligand-exchange process.[22] The resulting ChAM-NC dispersions are charge stabilized and cannot be readily assembled in the same manner as (sterically stabilized) hybrid colloidal NCs (Figure 2e). The advantage,
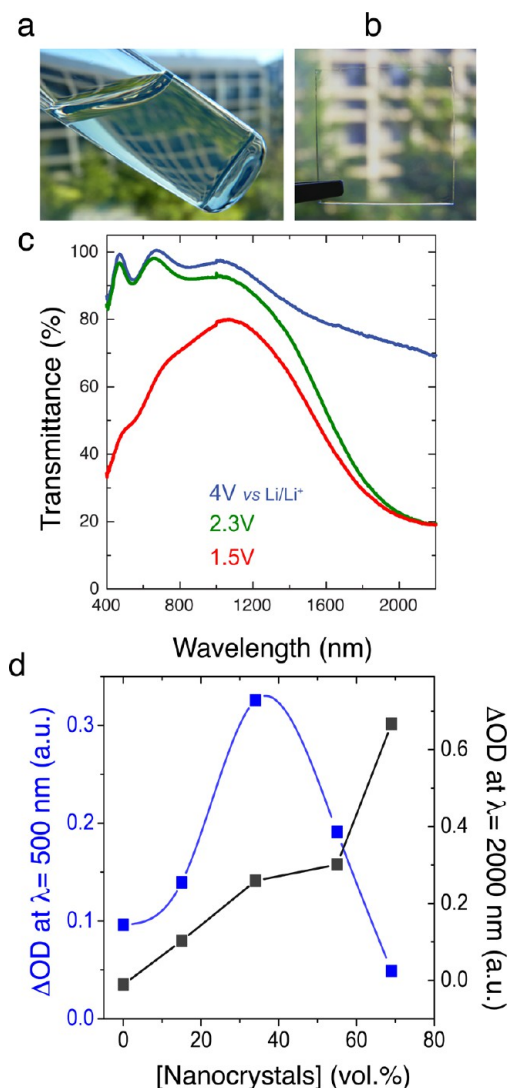
FIGURE 3. ITO-in-NbO$_x$ electrochromic composite films.[28] (a) Aqueous POM-stabilized dispersion of ITO NCs. (b) Transparent ITO-in-NbO$_x$ film obtained after solution deposition and thermal annealing. (c) Dual-band electrochromic response of an ITO-in-NbO$_x$ film. At oxidative voltages, the film is transparent to solar radiation, allowing heat and natural light to transmit through. Reducing the voltage to an intermediate value, the film switches to a NIR-blocking state, owing to plasmonic effects in the NCs. Lower potentials are needed to electrochemically reduce Nb^{5+} and induce the optical response of the matrix (visible range). (d) Change in optical density, at specified wavelengths, of ITO-in-NbO$_x$ films with increasing NC content. Adapted from ref 28. Copyright 2013 Nature Publishing Group.

however, is that the ex situ approach makes volume fraction readily tunable by adding a variable amount of excess cluster to the cluster-stabilized NC solution before film casting.

Solvent incompatibility becomes a major challenge when aiming to link highly charged water-soluble clusters, like POMs, to hydrophobic hybrid colloidal NCs. Our attempts to

exchange native ligands with POMs by a one-step process led to nonquantitative, irreproducible, and kinetically infeasible results. Pursuing a general ex situ method, we developed a two-step process in which NCs are first freed from their native ligands by reaction with NOBF$_4$ or Meerwein's salt, leaving open coordination sites at their naked, positively charged surfaces.[26] The Murray group introduced NOBF$_4$ as a reactive stripping agent,[30] which is highly effective for chemically robust inorganic compositions. However, many materials are etched or completely dissolved by NOBF$_4$ or its acidic byproducts. As an alternative, Meerwein's and related alkyloxonium salts are strong alkylating agents that render native ligands noncoordinating without disturbing the inorganic core of most NCs.[31] Thus, NCs synthesized by organic phase reactions can now generally be rendered ligand-free and their electrophilic surfaces made ready to form coordination bonds with secondary ligands of interest.[30,32]

The two-step exchange process yields POM-stabilized NC dispersions from which films can be deposited and then thermally annealed to make nanocrystal-in-glass composites (Figure 3, panels a and b). This ex situ approach is flexible, permitting us to choose combinations of components to tailor functionality. In addition, the direct bonding between NCs and the surrounding matrix constitutes an "active link" that plays a significant, if not dominant, role in determining the properties of the overall composite mesostructured material.

Reconstruction at heterogeneous interfaces can give rise to properties not characteristic of either bulk material. For instance, interface-induced nanostrain dramatically improved the superconducting transport properties of epitaxial YBa$_2$Cu$_3$O$_x$ films containing nonsuperconducting nano-inclusions.[33,34] Electronic reconstruction leading to enhanced electronic conductivity while reducing thermal conductivity amplifies thermoelectric performance when semimetal inclusions are epitaxially embedded in semiconductors.[35] Interface reconstruction can even create metallic electronic conductivity or extraordinarily high ionic conductivity at the boundary between insulators.[36,37] Reconstruction at glass−crystal interfaces has been less studied; nonetheless, intriguing examples of enhanced conductivity have been recently reported.[38,39] In mesostructured materials, the interfaces become sufficiently close to each other that they interact, so the properties of the material as a whole are strongly influenced by interface reconstruction.[40]

In Ag$_2$S-in-GeS$_2$ nanocrystal-in-glass materials made by in situ ligand exchange, we found the signature of interface effects on ionic conductivity.[27] In a mesostructural series, the
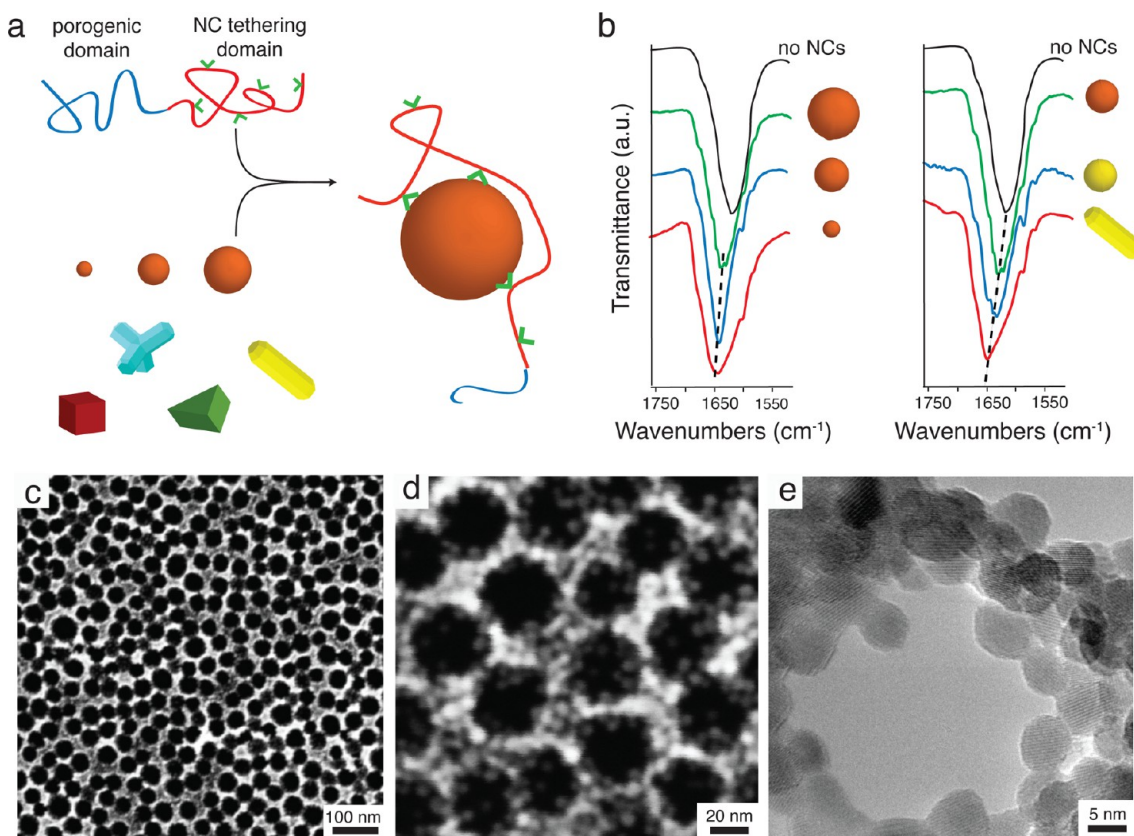
FIGURE 4. Mesoporous architectures constructed by enthalpy-driven assembly of NCs. (a) Co-assembly scheme of ligand-stripped NCs with purpose-made BCPs. (b) Fourier Transform Infrared spectra showing the shift of the PDMA amide carbonyl resonance in films obtained by combining PDMA-*b*-PS with different size ITO NCs (8, 6, and 4.5 nm) (left) or ITO versus TiO_2 NCs of same size (8 nm) and TiO_2 nanorods (3 by 20 nm) (right). (c) Top-view SEM of a mesoporous film of 4.5 nm ITO NCs. (d) High-resolution SEM and (e) TEM of the same. Adapted from ref 46. Copyright 2012 American Chemical Society.

Ag_2S NC size was varied while the thickness of the GeS_2 layer separating adjacent particles was constant, around 0.7 nm. The in situ process guarantees continuous Ag^+ ion transport pathways through GeS_2 glass immediately adjacent to Ag_2S NC surfaces. The ionic conductivity of these composites (assessed by impedance spectroscopy) is enhanced by more than an order of magnitude compared to pure Ag_2S. Analyzing the trends in ionic conductivity with thermal activation and with NC size suggested that interfacial transport, through the GeS_2 glass matrix, contributes substantially. This is a marked deviation from NC TFTs, which are proposed to carry electronic charge strictly by hopping between NCs even in the presence of a thin metal chalcogenide matrix.[17]

The contribution of the matrix material to the observed properties can be even greater when the ex situ ligand exchange approach is employed to increase the volume fraction of the matrix. For instance, introducing Ag nanoparticles into a Sb_2Te_3 matrix gave rise to Schottky barriers at the embedded interfaces and enhanced the thermoelectric power factor by 50% compared to pure Sb_2Te_3 (see ref 41).

Most recently, we showed that progressively tuning the matrix volume fraction by ex situ processing tuned the relative visible and near-infrared (NIR) optical modulation in composite electrochromic metal oxide films (Figure 3, panels c and d).[28] Visible light transmittance modulation derives from the reversible reduction of Nb^{5+} within the amorphous NbO_x matrix. Meanwhile, strong NIR transmittance modulation is afforded by the plasmonic electrochromism of ITO NCs[15], which are embedded in the NbO_x glass. Although the extent of NIR switching varies monotonically with the ITO volume fraction, a dramatic deviation from linearity is observed in the visible light modulation (Figure 3d). The absolute dynamic range is enhanced by more than three times and is correlated with an increase in the charge capacity. By Raman spectroscopy, we found that the bonding network of NbO_x is dramatically reconstructed by linking to the embedded NCs. Just as in the Ag_2S-in-GeS_2 composites, the thin (~0.7 nm) matrix material between closely spaced NCs provides effective ion transport channels, and the characteristics of the overall material are strongly perturbed by the percolation of NC−glass interfaces.
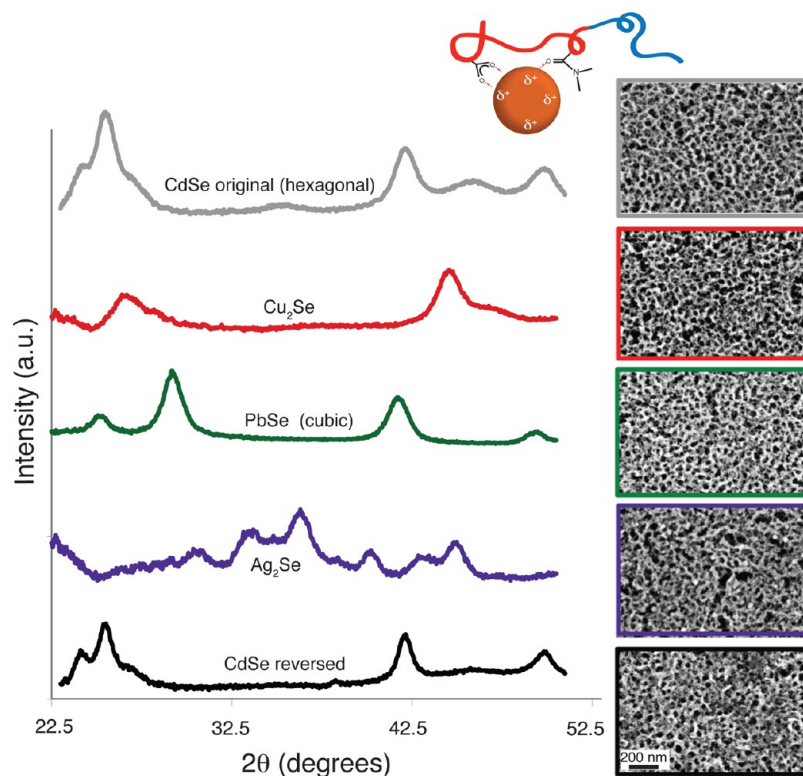
FIGURE 5. Cation exchange transformations of metal chalcogenide mesoporous architectures. X-ray diffraction patterns (left) and top-down SEM (right) of metal chalcogenide films obtained by cation-exchange reactions. PbSe and CdSe reversed samples were obtained after first exchanging to Cu_2Se. Cu_2Se and Ag_2Se films were reached directly from CdSe. Adapted from ref 47. Copyright 2013 American Chemical Society.

Arranging Nanocrystals in Mesoporous Architectures. Material properties derive not only from the arrangement of matter but also of open space. Just as for nanocrystal-in-matrix materials, using colloidal NCs as building blocks for mesoporous materials offers the benefit of flexible component selection (composition, size, and shape) well beyond that possible in conventional porous materials such as zeolites, templated sol−gel materials, or metal−organic frameworks.

Early work capitalized on the weak interactions between the hydroxylated surfaces of some metal oxide NCs and the polar poly(ethylene oxide) block of amphiphilic block copolymer (BCP) templating agents, yet these assemblies lacked order and pore dimensions were not well controlled.[42] Meanwhile, assembly of metal chalcogenide and metal phosphide NCs into random porous networks has been achieved by oxidation of the ligands to induce direct NC−NC interactions, but these again lack any regular mesostructure.[43,44] In one notable example, a highly ordered assembly of small (1.8 nm) Pt NCs was obtained by deliberately designing the BCP and NC ligands to enhance their enthalpy of interaction.[45] Nonetheless, a general route to assembling NCs synthesized through optimal, organic-phase colloidal chemistry has been lacking. We have recently demonstrated that these challenges can be resolved by stripping ligands[30,31] and designing BCPs that adsorb dynamically to the resulting open surface coordination sites.[46,47]

Our BCPs contain a NC tethering domain, poly(*N,N*-dimethylacrylamide) (PDMA, inspired by the ready dispersibility of naked NCs in *N,N*-dimethylformamide) and a nonpolar porogenic block, polystyrene (PS).[46] These polymers form micelles with PS cores and PDMA coronas. NCs decorate these micelles, a process driven by an adsorption enthalpy that overcomes NC−NC interactions and entropic penalties deriving from restricted polymer configuration. Compared to evaporation-induced assembly,[42,48,49] this supramolecular approach greatly improves the ordering of the resulting hierarchically porous NC films (Figure 4).[46] It is broadly applicable to NCs of diverse morphology (size and shape) and composition (from oxides to nanophosphors and metal alloys) and is tolerant of NC polydispersity. All critical length scales describing these architectures are synthetically tunable: nanocrystallite dimensions and phase are established through colloidal synthesis, while the mesopore dimensions and wall thickness are controlled through the molecular weight of the BCP porogenic domain and NC tethering domain, respectively.
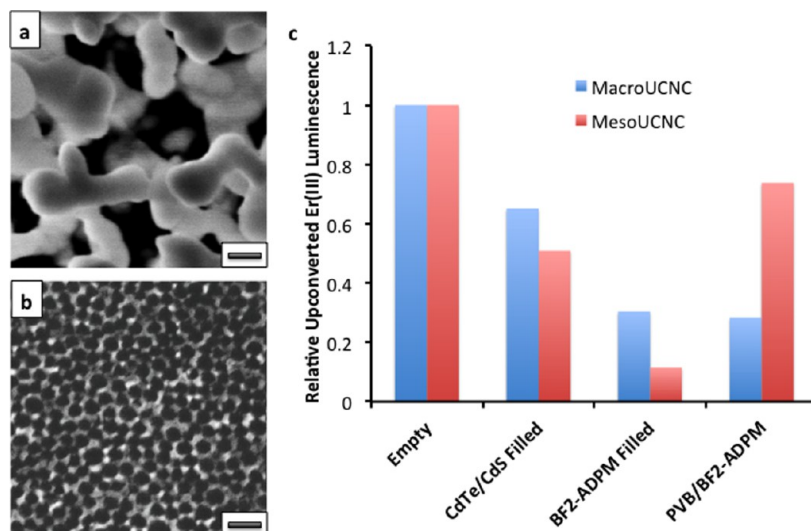
FIGURE 6. Size-selective infiltration of upconverting porous architectures. Top-down SEM of (a) macroporous and (b) mesoporous thin films constructed from the same NC building blocks. (c) The fraction of integrated Er^{3+} luminescence remaining after infiltration with various quenching agents. Panel (b) adapted from ref 46. Copyright 2012 American Chemical Society.

We found spectroscopic evidence for the tethering of NCs by PDMA in the shifted frequency of the amide carbonyl stretching vibration, which trends with NC size and composition (Figure 4b).[46] Recently, we extended this concept to construct ordered mesoporous films from metal chalcogenide materials. In this case, competition for surface coordination by *N,N*-dimethylformamide present in the dispersion necessitated the strengthening of BCP–NC interactions by randomly "doping" the PDMA with 10% poly(acrylic acid) (PAA) (Figure 5).[47]

The NC architectures we construct by this enthalpy-driven process are quite robust and can withstand significant strain arising from chemical transformations driven by ion insertion and extraction. In fact, TiO_2 nanorod-based mesoporous architectures are highly durable (>1000 cycles) under electrochemical cycling between lithiated and delithiated phases (about 3% strain).[46] Metal chalcogenide architectures can be transformed through complete replacement of their cations while retaining their mesoporous structure (Figure 5).[47]

Such regular mesoscale pores are selectively accessible for infiltration by exogenous components. To illustrate this, we followed the quenching of upconverted luminescence (visible emission following multiphoton NIR excitation) in lanthanide-doped macro- and mesoporous architectures upon infiltration by various energy transfer acceptors (Figure 6). Both films initially exhibited bright visible Er^{3+} luminescence under 980 nm excitation. Infiltrating the pores with colloidal CdTe/CdS core/shell NCs quenched the Er^{3+} luminescence to different degrees for the macro- and

mesoporous architectures: 35% and 49%, respectively. This suggests that, on average, the NC quenchers reside closer to emissive Er^{3+} in the higher-surface area mesoporous films. A similar trend in quenching efficacy was found after infiltrating with small molecule acceptors: red-absorbing azadipyrromethene dye BF2-ADPM,[50] quenched 89% of the Er^{3+} luminescence of the mesoporous architecture, compared to 70% for the macroporous films. Interestingly, when we mixed the dye with 20 kDa poly(vinyl butyral) (PVB), quenching of the macroporous upconverting luminescence was unchanged from that for the dye alone, while luminescence quenching of the mesoporous architecture was reduced to only 26%. This suggests that the controlled dimensions of the mesopores provide a selective cutoff that resists backfilling by larger molecular weight species such as the PVB. Meanwhile small molecules and few-nanometer diameter NCs readily infiltrate the mesoporous architecture and make direct contact with its large internal surface area.

Conclusion

Assembly of NCs into mesostructured materials began in the earliest days of synthesizing near monodisperse particles. However, the ligands facilitating these initial assembly methods have severely limited development of functional mesostructured materials. Recent advances in understanding and manipulation of NC surface chemistry have helped foment a burst of progress. NC surfaces can now reliably be stripped free of their native ligands, thus opening coordination sites for direct interaction with heterogeneous building

blocks ranging from inorganic clusters to purpose-made block copolymers. The resulting nanocomposite and mesoporous materials have enormous potential for new functionality. In particular, the direct linking of heterogeneous components offers unprecedented opportunities to generate materials whose characteristics derive from the constituents yet are also strongly modified by interfacial interactions. The combinations of properties that are possible in such mesoscale architectures are dizzying, suggesting new rules are needed that transcend design paradigms developed for crystalline bulk materials and for noninteracting nanostructures.

Outlook. This is an exciting time for mesostructured materials: new fabrication strategies have begun to empower systematic elucidation of design rules and deliberate elaboration of new functionality. Clearly, chemically bonding NCs to polymers and to inorganic clusters alike can effect reconstruction immediately adjacent to the NC surface and this restructuring plays an active role in determining properties of the resulting mesostructured materials. Given its central role, we must seek a deeper understanding of this active link. Advanced spectroscopies and microscopies will be applied to reveal how the material near the interface is physically and electronically modified and what complementary changes take place on the other side of the interface, within the NCs themselves.

In our work, we are particularly intrigued by the role that such interfaces can play in modifying ionic transport. Impedance analysis of granular solids has highlighted the dominant influence that grain boundaries can have on ionic conductivity. For instance, cerium oxide is a good ionic conductor and electronic insulator when prepared with large grains, yet these partial conductivities change by orders of magnitude when the grain size is reduced; nanocrystalline ceria is an *n*-type electronic conductor and relatively poor ionic conductor.[51,52] Related effects arise from heterogeneous interfaces in superlattices prepared by molecular beam epitaxy.[37,40] Ionic conductivities can be enhanced by 7 orders of magnitude in such constructs. If similar behavior could be harnessed in nanocrystal-in-matrix composites, then a new breed of heterogeneous electrochemical materials could emerge whose properties hinge on their mesostructure as well as their composition. However, to quantitatively understand the emergence of interface-derived function, we must evaluate changes in conductivities and other properties while the mesostructured architecture is varied in a well-controlled fashion, for example by varying the interfacial area at a fixed volume fraction.

Finally, the vast opportunities to manipulate function through interfacial interactions will stimulate the introduction of additional compositional heterogeneity while maintaining order so that the mechanisms underlying emergent properties can be rationalized. For example, multicomponent NC superlattices[4,6] could be embedded in active inorganic matrices by in situ ligand exchange.[23] Mesoporous architectures can be infiltrated with species lending complementary functionality to channel the migration of energy and charge. Heterogeneous porous architectures could be constructed by using purpose-made BCPs to simultaneously direct the arrangement of two types of NCs or of NCs and inorganic clusters. Ultimately, we could deliberately arrange multiple inorganic components and open spaces in endless combinations. The mutual influence of each element on the others will be the rivets and beams from which we construct functional materials in the future.

BIOGRAPHICAL INFORMATION

Delia J. Milliron was born in Niskayuna, New York, in 1977. She received her A.B. (1999) from Princeton University and her Ph.D. (2004) with A. Paul Alivisatos at the University of California, Berkeley. She held positions at IBM's Watson and Almaden Research Centers before joining the staff of the Molecular Foundry at Lawrence Berkeley National Laboratory in 2008. Her current research interests include plasmonic semiconductor nanocrystals, assembly of heterogeneous mesostructured materials, and the electrochemical properties of both.

Raffaella Buonsanti was born in Tricarico (MT), Italy, in 1981. She received her M.S. (2006) from University of Bari (Italy) and her Ph.D. (2010) with P. Davide Cozzoli at the National Nanotechnology Laboratory, University of Salento, Lecce (Italy). In 2010, she joined the Milliron research group as a postdoctoral fellow before joining the staff of the Molecular Foundry in 2012. Her research interests include doped nanocrystals, multifunctional nanocrystalline heterostructures, and their assembly for photocatalytic applications.

Anna Llordés Gil was born in Terrassa, Barcelona (Spain), in 1978. She received her B.S. in chemistry (2002) from Universitat Autònoma de Barcelona and her Ph.D. (2010) at the Institut de Ciència de Materials de Barcelona (ICMAB-CSIC) supervised by X. Obradors and S. Ricart. In 2010, she joined the Milliron research group as a postdoctoral fellow and is now a Project Scientist. Her research interests include chemical approaches to assemble mesostructured composites, characterization of interface reconstruction, and mesostructure–property relationships of metal oxide materials.

Brett A. Helms was born in Richmond, California, in 1978. He received his B.S. (2000) from Harvey Mudd College and his Ph.D. (2006) with Jean M. J. Fréchet at the University of California, Berkeley. He joined the staff of the Molecular Foundry in 2007, after postdoctoral research at the Technische Universiteit

Eindhoven with E. W. (Bert) Meijer. His research interests include structure of and reactivity at nanocrystal surfaces and assembly of functional mesomaterial systems.

REFERENCES

1 Murray, C. B.; Norris, D. J.; Bawendi, M. G. Synthesis and Characterization of Nearly Monodisperse CdE (E = S, Se, Te) Semiconductor Nanocrystallites. *J. Am. Chem. Soc.* **1993**, *115*, 8706–8715.

2 Murray, C. B.; Kagan, C. R.; Bawendi, M. G. Three-Dimensional Quantum Dot Superlattices. *Science* **1995**, *270*, 1335–1338.

3 Redl, F. X.; Cho, K.-S.; Murray, C. B.; O'Brien, S. Three-Dimensional Binary Superlattices of Magnetic Nanocrystals and Semiconductor Quantum Dots. *Nature* **2003**, *423*, 968–971.

4 Shevchenko, E. V.; Talapin, D. V.; Kotov, N. A.; O'Brien, S.; Murray, C. B. Structural Diversity in Binary Nanoparticle Superlattices. *Nature* **2006**, *439*, 55–59.

5 Bodnarchuk, M. I.; Kovalenko, M. V.; Heiss, W.; Talapin, D. V. Energetic and Entropic Contributions to Self-Assembly of Binary Nanocrystal Superlattices: Temperature as the Structure-Directing Factor. *J. Am. Chem. Soc.* **2010**, *132*, 11967–11977.

6 Evers, W. H.; Friedrich, H.; Filion, L.; Dijkstra, M.; Vanmaelkelbergh, D. Observation of a Ternary Nanocrystal Superlattice and Its Structural Characterization by Electron Tomography. *Angew. Chem., Int. Ed.* **2009**, *48*, 9655–9657.

7 Pileni, M. P. Nanocrystal Self-Assemblies: Fabrication and Collective Properties. *J. Phys. Chem. B* **2001**, *105*, 3358–3371.

8 Pileni, M. P. Supracrystals of Inorganic Nanocrystals: An Open Challenge for New Physical Properties. *Acc. Chem. Res.* **2008**, *41*, 1799–1809.

9 Baker, J. L.; Widmer-Cooper, A.; Toney, M. F.; Geissler, P. L.; Alivisatos, A. P. Device-Scale Perpendicular Alignment of Colloidal Nanorods. *Nano Lett.* **2010**, *10*, 195–201.

10 Black, C. T.; Murray, C. B.; Sandstrom, R. L.; Sun, S. Spin-Dependent Tunneling in Self-Assembled Cobalt-Nanocrystal Superlattices. *Science* **2000**, *290*, 1131–1134.

11 Talapin, D. V.; Murray, C. B. PbSe Nanocrystal Solids for n- and p-Channel Thin Film Field-Effect Transistors. *Science* **2005**, *310*, 86–89.

12 Ridley, B. A.; Nivi, B.; Jacobson, J. M. All-Inorganic Field Effect Transistors Fabricated by Printing. *Science* **2000**, *286*, 746–749.

13 Pattantyus-Abraham, A. G.; Kramer, I. J.; Barkhouse, A. R.; Wang, X.; Konstantatos, G.; Debnath, R.; Levina, L.; Raabe, I.; Nazeeruddin, M. K.; Gratzel, M.; Sargent, E. H. Depleted-Heterojuntion Colloidal Quantum Dot Solar Cells. *ACS Nano* **2010**, *4*, 3374–3380.

14 Gur, I.; Fromer, N. A.; Geier, M. L.; Alivisatos, A. P. Air-Stable All-Inorganic Nanocrystal Solar Cells Processed from Solution. *Science* **2005**, *310*, 462–465.

15 Garcia, G.; Buonsanti, R.; Runnerstrom, E. L.; Mendelsberg, R. J.; Llordes, A.; Anders, A.; Richardson, T. J.; Milliron, D. J. Dynamically Modulating the Surface Plasmon Resonance of Doped Semiconductor Nanocrystals. *Nano Lett.* **2011**, *11*, 4415–4420.

16 Garcia, G.; Buonsanti, R.; Llordes, A.; Runnerstrom, E. L.; Bergerud, A.; Milliron, D. J. Near Infrared Spectrally Selective Plasmonic Electrochromic Thin Films. *Adv. Opt. Mater.* **2013**, *1*, 215–220.

17 Choi, J.-H.; Fafarman, A. T.; Oh, S. J.; Ko, D.-K.; Kim, D. K.; Diroll, B. T.; Muramoto, S.; Gillen, J. G.; Murray, C. B.; Kagan, C. R. Bandlike Transport in Strongly Coupled and Doped Quantum Dot Solids: A Route to High-Performance Thin-Film Electronics. *Nano Lett.* **2012**, *12*, 2631–2638.

18 Lee, J.-S.; Kovalenko, M. V.; Huang, J.; Chung, D. S.; Talapin, D. V. Band-Like Transport, High Electron Mobility and High Photoconductivity in All-Inorganic Nanocrystal Arrays. *Nat. Nanotechnol.* **2011**, *6*, 348–352.

19 Dehnen, S.; Melullis, M. A Coordination Chemistry Approach Towards Ternary M/14/16 Anions. *Coord. Chem. Rev.* **2007**, *251*, 1259–1280.

20 Haddadpour, S.; Melullis, M.; Staesche, H.; Mariappan, C. R.; Roling, B.; Rodolphe, C.; Dehnen, S. Inorganic Frameworks from Selenidotetrelate Anions $[T_2Se_6]^{4-}$ (T=Ge, Sn): Synthesis, Structures, and Ionic Conductivity of $[K_2(H_2O)_3][MnGe_4Se_{10}]$ and $(NMe_4)_2[MSn_4Se_{10}]$ (M=Mn, Fe). *Inorg. Chem.* **2009**, *48*, 1689–1698.

21 Mitzi, D. B.; Kosbar, L. L; Murray, C. E.; Copel, M.; Afzali, A. High-Mobility Ultrathin Semiconducting Films Prepared by Spin Coating. *Nature* **2004**, *428*, 299–303.

22 Kovalenko, M. V.; Scheele, M.; Talapin, D. V. Colloidal Nanocrystals with Molecular Metal Chalcogenide Surface Ligands. *Science* **2009**, *324*, 1417–1420.

23 Tangirala, R.; Baker, J. L.; Alivisatos, A. P.; Milliron, D. J. Modular Inorganic Nanocomposites by Conversion of Nanocrystal Superlattices. *Angew. Chem., Int. Ed.* **2010**, *49*, 2878–2882.

24 Danek, M.; Jensen, K. F.; Murray, C. B.; Bawendi, M. G. Electrospray Organometallic Chemical Vapor Deposition: A Novel Technique for Preparation of II-VI Quantum Dot Composites. *Appl. Phys. Lett.* **1994**, *65*, 2795–2797.

25 Woggon, U.; Herz, E.; Schops, O.; Artemyev, M. V.; Arens, Ch.; Rousseau, N.; Schikora, D.; Lischka, K.; Litvinov, D.; Gerthsen, D. Hybrid Epitaxial-Colloidal Semiconductor Nanostructures. *Nano Lett.* **2005**, *5*, 483–490.

26 Llordes, A.; Hammack, A. T.; Buonsanti, R.; Tangirala, R.; Aloni, S.; Helms, B. A.; Milliron, D. J. Polyoxometalates and Colloidal Nanocrystals as Building Blocks for Metal Oxide Nanocomposite Films. *J. Mater. Chem.* **2011**, *21*, 11631–11638.

27 Wang, R. Y.; Tangirala, R.; Raoux, S.; Jordan-Sweet, J. L.; Milliron, D. J. Ionic and Electronic Transport in Ag_2S Nanocrystal-GeS_2 Matrix Composites with Size-Controlled Ag_2S Nanocrystals. *Adv. Mater.* **2012**, *24*, 99–103.

28 Llordes, A.; Garcia, G.; Gazquez, J.; Milliron, D. J. Tunable Near-Infrared and Visible Light Transmittance in Nanocrystal-in-Glass Composites. *Nature* **2013**, *500*, 323–326.

29 Sakamoto, A.; Yamamoto, S. Glass—Ceramics: Engineering Principles and Applications. *Int. J. Appl. Glass Sci.* **2010**, *1*, 237–247.

30 Dong, A.; Ye, X.; Chen, J.; Kang, Y.; Gordon, T.; Kikkawa, J. M.; Murray, C. B. A Generalized Ligand-Exchange Strategy Enabling Sequential Surface Functionalization of Colloidal Nanocrystals. *J. Am. Chem. Soc.* **2011**, *133*, 998–1006.

31 Rosen, E. L.; Buonsanti, R.; Llordes, A.; Sawvel, A. M.; Milliron, D. J.; Helms, B. A. Exceptionally Mild Reactive Stripping of Native Ligands from Nanocrystal Surfaces Using Meerwein's Salt. *Angew. Chem., Int. Ed.* **2012**, *51*, 684–689.

32 Duong, J. T.; Bailey, M. J.; McBride, P. M.; Buonsanti, R.; Pick, T. E.; Rosen, E. L.; Milliron, D. J.; Helms, B. A. Efficient Polymer Passivation of Ligand-Stripped Nanocrystal Surfaces. *J. Poly. Sci. A: Poly. Chem.* **2012**, *50*, 3719–3727.

33 Macmanus-Driscoll, J. L.; Foltyn, S. R.; Jia, Q. X.; Wang, H.; Serquis, A.; Civale, L.; Maiorov, B.; Hawley, M. E.; Maley, M. P.; Peterson, D. E. Strongly Enhanced Current Densities in Superconducting Coated Conductors of $YBa_2Cu_3O_{7-x}+BaZrO_3$. *Nat. Mater.* **2004**, *3*, 439–443.

34 Llordés, A.; Palau, A.; Gazquez, J.; Coll, M.; Vlad, R.; Pomar, A.; Arbiol, J.; Guzman, R.; Ye, S.; Ruoco, V.; Sandiumenge, F.; Ricart, S.; Puig, T.; Varela, M.; Chateigner, D.; Vanacken, J.; Gutierrez, J.; Moshchalkov, V.; Deutscher, G.; Magen, C.; Obradors, X. Nanoscale Strain-Induced Pair Suppression as a Vortex-Pinning Mechanism in High-Temperature Superconductors. *Nat. Mater.* **2012**, *11*, 329–336.

35 Zide, J. M.; Klenov, D. O.; Stemmer, S.; Gossard, A. C.; Zeng, G.; Bowers, J. E.; Vashaee, D.; Shakouri, A. Thermoelectric Power Factor in Semiconductors with Buried Epitaxial Semimetallic Nanoparticles. *Appl. Phys. Lett.* **2005**, *87*, 112102-1–112103-3.

36 Okamoto, S.; Millis, A. J. Electronic Reconstruction at an Interface between a Mott Insulator and a Band Insulator. *Nature* **2004**, *428*, 630–633.

37 Garcia-Barriocanal, J.; Rivera-Calzada, A.; Varela, M.; Sefrioui, Z.; Iborra, E.; Leon, C.; Pennycook, S. J.; Santamaria, J. Colossal Ionic Conductivity at Interfaces of Epitaxial ZrO_2: $Y_2O_3/SrTiO_3$ Heterostructures. *Science* **2008**, *321*, 676–680.

38 Chen, Y.; Pryds, N.; Kleibeuker, J. E.; Koster, G.; Sun, J.; Stamate, E.; Shen, B.; Rijnders, G.; Linderoth, S. Metallic and Insulating Interfaces of Amorphous $SrTiO_3$-Based Oxide Heterostructures. *Nano Lett.* **2011**, *11*, 3774–3778.

39 Lee, S. W.; Liu, Y.; Heo, J.; Gordon, R. G. Creation and Control of Two-Dimensional Electron Gas Using Al-Based Amorphous Oxides/$SrTiO_3$ Heterostructures Grown by Atomic Layer Deposition. *Nano Lett.* **2012**, *12*, 4775–4783.

40 Sata, N.; Eberman, K.; Maier, J. Mesoscopic Fast Ion Conduction in Nanometre-Scale Planar Heterostructures. *Nature* **2000**, *408*, 946–949.

41 Zhang, Y.; Snedaker, M. L.; Birkel, C. S.; Mubeen, S.; Ji, X.; Shi, Y.; Liu, D.; Liu, X.; Moskovits, M.; Stucky, G. D. Silver-Based Intermetallic Heterostructures in Sb_2Te_3 Thick Films with Enhanced Thermoelectric Power Factors. *Nano Lett.* **2012**, *12*, 1075–1080.

42 Brezesinski, T.; Wang, J.; Polleux, J.; Dunn, B.; Tolbert, S. H. Templated Nanocrystal-Based Porous TiO_2 Films for Next-Generation Electrochemical Capacitors. *J. Am. Chem. Soc.* **2009**, *131*, 1802–1809.

43 Mohanan, J. L.; Arachchige, I. U.; Brock, S. L. Porous Semiconductor Chalcogenide Aerogels. *Science* **2005**, *307*, 397–400.

44 Hitihami-Mudiyanselage, A.; Senevirathne, K.; Brock, S. L. Assembly of Phosphide Nanocrystals into Porous Networks: Formation of InP Gels and Aerogels. *ACS Nano* **2013**, *7*, 1163–1170.

45 Warren, S. C.; Messina, L. C.; Slaughter, L. S.; Kamperman, M.; Zhou, Q.; Gruner, S. M.; DiSalvo, F. J.; Wiesner, U. Ordered Mesoporous Materials from Metal Nanoparticle-Block Copolymer Self-Assembly. *Science* **2008**, *320*, 1748–1752.

46 Buonsanti, R.; Pick, T. E.; Krins, N.; Richardson, T. J.; Helms, B. A.; Milliron, D. J. Assembly of Ligand-Stripped Nanocrystals into Precisely Controlled Mesoporous Architectures. *Nano Lett.* **2012**, *12*, 3872–3877.

47 Rivest, J. B.; Buonsanti, R.; Pick, T. E.; Zhu, L.; Lim, E.; Clavero, C.; Schaible, E.; Helms, B. A.; Milliron, D. J. Evolution of Ordered Metal Chalcogenide Architectures through Chemical Transformations. *J. Am. Chem. Soc.* **2013**, *135*, 7446–7449.

48 Rauda, I. E.; Buonsanti, R.; Saldarriaga-Lopez, L. C.; Benjauthrit, K.; Schelhas, L. T.; Stefik, M.; Augustyn, V.; Ko, J.; Dunn, B.; Wiesner, U.; Milliron, D. J.; Tolbert, S. H. General Method for the Synthesis of Hierarchical Nanocrystal-Based Mesoporous Materials. *ACS Nano* **2012**, *6*, 6386–6399.

49 Rauda, I. E.; Saldarriaga-Lopez, L. C.; Helms, B. A.; Schelhas, L. T.; Membreno, D.; Milliron, D. J.; Tolbert, S. H. Nanoporous Semiconductors Synthesized through Polymer Templating of Ligand-Stripped CdSe Nanocrystals. *Adv. Mater.* **2013**, *25*, 1315–1322.

50 Leblebici, S. Y.; Catane, L.; Barclay, D. E.; Olson, T.; Chen, T. L.; Ma, B. Near-Infrared Azadipyrromethenes as Electron Donor for Efficient Planar Heterojunction Organic Solar Cells. *ACS Appl. Mater. Interfaces* **2011**, *3*, 4469–4474.

51 Chiang, Y.-M.; Lavik, E. B.; Kosacki, I.; Tuller, H. L.; Ying, J. Y. Nonstoichiometry and Electrical Conductivity of Nanocrystalline CeO_{2-x}. *J. Electroceram.* **1997**, *1*, 7–14.

52 Kim, S.; Maier, J. On the Conductivity Mechanism of Nanocrystalline Ceria. *J. Electrochem. Soc.* **2002**, *149*, J73–J83.